

# Journal of Mechanics of Materials and Structures

INTERACTION OF SHEAR CRACKS IN  
MICROSTRUCTURED MATERIALS MODELED BY  
COUPLE-STRESS ELASTICITY

Panos A. Gourgiotis

Volume 13, No. 3

May 2018



## INTERACTION OF SHEAR CRACKS IN MICROSTRUCTURED MATERIALS MODELED BY COUPLE-STRESS ELASTICITY

PANOS A. GOURGIOTIS

The interaction of two colinear in-plane shear cracks is investigated within the context of couple-stress elasticity. This theory introduces characteristic material length scales that emerge from the underlying microstructure and has proved to be very effective for modeling complex microstructured materials. An exact solution of the boundary value problem is obtained through integral transforms and singular integral equations. The main goal is to explain the size effects that are experimentally observed in fracture of brittle microstructured materials. Two basic configurations are considered: a micro-macrocrack interaction, and a micro-microcrack interaction. Numerical results are presented illustrating the effects of couple-stresses on the stress intensity factor and the energy release rate. It is shown that significant deviations from the predictions of the standard LEFM occur when the geometrical lengths of the problem become comparable to the characteristic material length of the couple-stress theory revealing that in such cases it is inadequate to analyze fracture problems employing only classical elasticity considerations.

### 1. Introduction

It is well known that in brittle materials crack growth is accompanied by the formation of microcracks around the main crack [Hoagland et al. 1974; Atkinson 1984; Rice et al. 1994; Nara et al. 2011]. The occurrence of such stress-induced microcracking has been recognized as an important toughening mechanism in many microstructured materials [Kreher and Pompe 1981; Evans and Faber 1984; Noselli et al. 2013]. There are many fracture models that deal with the nucleation and growth of such microcracks (e.g., [Kachanov 1993; Deng and Nemat-Nasser 1994; Shao and Rudnicki 2000]), however the majority of such models are based on the classical theory of linear elastic fracture mechanics (LEFM) which, however, is scale independent and cannot realistically describe the fracture processes in such situations. This deficiency of the classical theory can be circumvented by the use of generalized continuum theories. These theories introduce characteristic material lengths in their formulation and have been successfully employed in many cases to model the experimentally observed size-effects which are closely related to the material microstructure.

The simplest gradient-type generalized continuum theory that can effectively model size effects in elastic solids is the theory of couple-stress elasticity, also known as constrained Cosserat elasticity [Toupin 1962; Mindlin and Tiersten 1962; Koiter 1964]. In couple-stress elasticity the Euler–Cauchy principle is augmented with a nonvanishing couple traction and the strain-energy density becomes a function of the strain and the gradient of rotation. Such assumptions are appropriate for materials with granular or cellular structure, where the interaction between adjacent elements may introduce internal moments. For

*Keywords:* Cosserat media, energy release rate, micro-macrocrack interaction, crack shielding, microstructure.

the plane-strain isotropic case, the couple-stress theory introduces one material length scale which can be related to the intrinsic material microstructure [Lakes 1983; Anderson and Lakes 1994; Bigoni and Drugan 2007; Lakes 2016]. The couple-stress theory has been recently employed to model size effects in microstructured materials in, among other areas, fracture [Gourgiotis and Georgiadis 2008; Radi 2008; Piccolroaz et al. 2012; Gourgiotis and Piccolroaz 2014; Morini et al. 2014; Dyskin and Pasternak 2015], contact [Zisis et al. 2014; 2015; Gourgiotis et al. 2016; Karuriya and Bhandakkar 2017; Song et al. 2017; Wang et al. 2018], stress localization [Gourgiotis and Bigoni 2016a; 2016b; Bigoni and Gourgiotis 2016; Zisis 2018; Lakes 2018], and wave propagation problems [Piccolroaz and Movchan 2014; Goodarzi et al. 2016; Wang et al. 2017; Gourgiotis and Bigoni 2017].

The present work examines the interaction problem of two shear cracks in a microstructured material under remote mode II loading. The material microstructure is modeled here by use of the couple-stress theory. For simplicity, the attention here is limited to the case of two colinear finite-length cracks in an infinite body under plane-strain conditions. Of special interest is the case where the geometrical lengths of the problem become comparable to the characteristic material length of the couple-stress theory. In this context, two configurations are examined in detail: the micro-macrocrack interaction; and the micro-microcrack interaction. In the framework of the classical LEFM theory, crack interaction problems were investigated, among others, in [Rubinstein 1985; Rose 1986; Kachanov 1993; Deng and Nemat-Nasser 1994]. Interestingly, the crack interaction problem has not been investigated before in the context of any generalized continuum theory. Regarding works closely related to our problem, we cite first the analyses by Sternberg and Muki [1967] and Atkinson and Leppington [1977] who examined the mode I crack in a couple stress material. The full field solution for the mode II crack problem in couple-stress elasticity was given by Gourgiotis and Georgiadis [2007], while recently Baxevanakis et al. [2017] examined the interaction problem of an in-plane shear crack with a glide dislocation.

A full field exact solution of the mixed boundary value problem is obtained by means of the Fourier transform and singular integral equations. Analytical expressions for the stress intensity factor (SIF) and the energy release rate (ERR) are obtained for both cracks. The dependence of these quantities upon the characteristic material length of the couple-stress theory is then examined in detail in order to assess the effects of the microstructure on the fracture process. A comparison of these quantities in the framework of couple-stress elasticity with the classical elasticity solutions is also provided. The main goal of the present study is to examine the possible deviations from the predictions of classical LEFM with a view towards understanding the mechanisms that govern the fracture of brittle materials on the microscale.

## 2. Basic equations of plane-strain couple-stress elasticity

In this section, we recall briefly the main features of the plane strain couple-stress elasticity. A detailed presentation of the plane strain anisotropic couple-stress theory can be found in [Gourgiotis and Bigoni 2017].

For a body that occupies a domain in the  $(x, y)$ -plane under conditions of plane-strain, the equations of equilibrium in the absence of body forces and body moments reduce to

$$\frac{\partial \sigma_{xx}}{\partial x} + \frac{\partial \sigma_{yx}}{\partial y} = 0, \quad \frac{\partial \sigma_{xy}}{\partial x} + \frac{\partial \sigma_{yy}}{\partial y} = 0, \quad \sigma_{xy} - \sigma_{yx} + \frac{\partial m_{xz}}{\partial x} + \frac{\partial m_{yz}}{\partial y} = 0, \quad (1)$$

where  $(\sigma_{xx}, \sigma_{yy}, \sigma_{xy}, \sigma_{yx})$  and  $(m_{xz}, m_{yz})$  are the nonvanishing components of the (asymmetric) stress and couple-stress tensors, respectively. The complete solution of (1) admits the following representation in terms of two sufficiently smooth stress functions  $\Phi(x, y)$  and  $\Psi(x, y)$  [Mindlin 1963]:

$$\begin{aligned}\sigma_{xx} &= \frac{\partial^2 \Phi}{\partial y^2} - \frac{\partial^2 \Psi}{\partial x \partial y}, & \sigma_{yy} &= \frac{\partial^2 \Phi}{\partial x^2} + \frac{\partial^2 \Psi}{\partial x \partial y}, \\ \sigma_{xy} &= -\frac{\partial^2 \Phi}{\partial x \partial y} - \frac{\partial^2 \Psi}{\partial y^2}, & \sigma_{yx} &= -\frac{\partial^2 \Phi}{\partial x \partial y} + \frac{\partial^2 \Psi}{\partial x^2},\end{aligned}\quad (2)$$

and

$$m_{xz} = \frac{\partial \Psi}{\partial x}, \quad m_{yz} = \frac{\partial \Psi}{\partial y}. \quad (3)$$

Accordingly, the governing kinematic relations in the framework of the geometrically linear theory become

$$\varepsilon_{xx} = \frac{\partial u_x}{\partial x}, \quad \varepsilon_{yy} = \frac{\partial u_y}{\partial y}, \quad \varepsilon_{xy} = \varepsilon_{yx} = \frac{1}{2} \left( \frac{\partial u_y}{\partial x} + \frac{\partial u_x}{\partial y} \right), \quad (4)$$

$$\omega = \frac{1}{2} \left( \frac{\partial u_y}{\partial x} - \frac{\partial u_x}{\partial y} \right), \quad \kappa_{xz} = \frac{\partial \omega}{\partial x}, \quad \kappa_{yz} = \frac{\partial \omega}{\partial y}, \quad (5)$$

where  $u_q$  are the displacement components,  $\varepsilon_{pq}$  are the components of the usual strain tensor,  $\omega_z \equiv \omega$  is the rotation, and  $(\kappa_{xz}, \kappa_{yz})$  are the nonvanishing components of the curvature tensor (i.e., the gradient of rotation) expressed in dimensions of [length]<sup>-1</sup>.

For a homogeneous centrosymmetric and isotropic couple-stress material the constitutive equations furnish

$$\sigma_{xx} = (\lambda + 2\mu)\varepsilon_{xx} + \lambda\varepsilon_{yy}, \quad \sigma_{yy} = (\lambda + 2\mu)\varepsilon_{yy} + \lambda\varepsilon_{xx}, \quad \sigma_{xy} + \sigma_{yx} = 4\mu\varepsilon_{xy} \quad (6)$$

and

$$m_{xz} = 4\mu\ell^2\kappa_{xz}, \quad m_{yz} = 4\mu\ell^2\kappa_{yz}, \quad (7)$$

where  $(\mu, \lambda)$  stand for the Lamé moduli, and  $\ell$  is the characteristic material length of couple-stress theory [Mindlin and Tiersten 1962]. Note also that  $\lambda = 2\mu\nu(1 - 2\nu)^{-1}$ , where  $\nu$  is the Poisson's ratio.

The Mindlin's stress functions must satisfy the following pair of differential equations that result from the requirement of kinematical compatibility [Muki and Sternberg 1965]:

$$\begin{aligned}\frac{\partial}{\partial x}(\Psi - \ell^2\nabla^2\Psi) &= -2(1 - \nu)\ell^2\nabla^2\left(\frac{\partial\Phi}{\partial y}\right), \\ \frac{\partial}{\partial y}(\Psi - \ell^2\nabla^2\Psi) &= 2(1 - \nu)\ell^2\nabla^2\left(\frac{\partial\Phi}{\partial x}\right),\end{aligned}\quad (8)$$

which, in turn, implies that

$$\nabla^4\Phi = 0, \quad \nabla^2\Psi - \ell^2\nabla^4\Psi = 0. \quad (9)$$

Finally, combining (2)–(7), one can obtain the following relations expressing the displacement gradients in terms of Mindlin’s stress functions:

$$\frac{\partial u_x}{\partial x} = \frac{1}{2\mu} \left( \frac{\partial^2 \Phi}{\partial y^2} - \frac{\partial^2 \Psi}{\partial x \partial y} - \nu \nabla^2 \Phi \right), \tag{10}$$

$$\frac{\partial u_y}{\partial y} = \frac{1}{2\mu} \left( \frac{\partial^2 \Phi}{\partial x^2} + \frac{\partial^2 \Psi}{\partial x \partial y} - \nu \nabla^2 \Phi \right), \tag{11}$$

$$\frac{\partial u_x}{\partial y} + \frac{\partial u_y}{\partial x} = -\frac{1}{2\mu} \left( 2 \frac{\partial^2 \Phi}{\partial x \partial y} - \frac{\partial^2 \Psi}{\partial x^2} + \frac{\partial^2 \Psi}{\partial y^2} \right). \tag{12}$$

### 3. Formulation of the crack problem

Consider two collinear cracks situated along the  $x$ -axis consisting of the segments  $\mathcal{L}_1 = (a_1 < x < b_1)$  and  $\mathcal{L}_2 = (a_2 < x < b_2)$ , with  $a_2 > b_1$  (Figure 1). The crack-faces are traction free and the body is subjected to remote mode II loading of magnitude  $S$ . For simplicity, the origin of the Cartesian coordinate system coincides with crack-tip  $a_1$ .

To facilitate our parametric analysis the following geometric quantities are defined

$$\alpha = \frac{1}{2}(b_1 - a_1), \quad \beta = \frac{1}{2}(b_2 - a_2), \quad \text{and} \quad \delta = a_2 - b_1, \tag{13}$$

where  $\alpha$  and  $\beta$  are the half-lengths of the two collinear cracks, and  $\delta$  is the distance between them.

Due to the antisymmetry with respect to the  $y = 0$  plane, the problem can be viewed as a half-plane problem in the domain  $y \geq 0$  under the following boundary conditions:

$$\sigma_{yx}(x, 0) = 0 \quad \text{for} \quad x \in \mathcal{L}, \tag{14}$$

$$\sigma_{yy}(x, 0) = 0 \quad \text{for} \quad -\infty < x < \infty, \tag{15}$$

$$m_{yz}(x, 0) = 0 \quad \text{for} \quad -\infty < x < \infty, \tag{16}$$

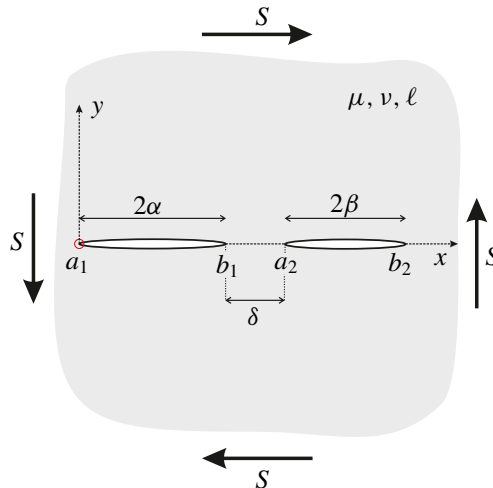


**Figure 1.** Two collinear cracks subjected to remote mode II loading.

accompanied by the antisymmetry condition

$$u_x(x, 0) = 0 \quad \text{for } x \notin \mathcal{L}, \tag{17}$$

and the regularity conditions at infinity

$$\sigma_{xy}^\infty = \sigma_{yx}^\infty = S, \quad \{\sigma_{xx}^\infty, \sigma_{yy}^\infty, m_{xz}^\infty, m_{yz}^\infty\} \rightarrow 0 \quad \text{as } r = \sqrt{x^2 + y^2} \rightarrow \infty, \tag{18}$$

with  $\mathcal{L} = \sum_{j=1}^2 \mathcal{L}_j$ .

Further, as it is customary in the classical theory of elasticity, we introduce the unknown density  $h(x)$  as the slope function

$$h(x) = \frac{\partial u_x(x)}{\partial x}, \tag{19}$$

which in view of (17), is defined as

$$h(x) = \begin{cases} h_j(x) & \text{for } x \in \mathcal{L}_j \ (j = 1, 2), \\ 0 & \text{for } x \notin \mathcal{L}. \end{cases} \tag{20}$$

For the solution of the boundary value problem the Fourier transform is utilized to suppress the  $x$ -dependence in the field equations and the boundary conditions. The direct and inverse Fourier transforms are defined as follows:

$$f^*(\xi, y) = \int_{-\infty}^{+\infty} f(x, y)e^{i\xi x} dx, \quad f(x, y) = \frac{1}{2\pi} \int_{-\infty}^{+\infty} f^*(\xi, y)e^{-i\xi x} d\xi, \tag{21}$$

where  $\xi$  is the Fourier variable and  $i$  is the imaginary unit. Transforming the governing field equations (9) provides a pair of fourth order ODEs with constant coefficients whose solution is immediate [Zisis et al. 2014]. The constants that emerge may be subsequently evaluated from the transform of (8) in conjunction with the boundary conditions (15) and (16). Finally, utilizing (10) and (19), the transformed stress functions assume the following form:

$$\Phi^*(\xi, y) = -\frac{\mu}{(1-\nu)} \frac{e^{-|\xi|y}}{|\xi|} h^*(\xi), \quad \Psi^*(\xi, y) = 4i\mu\ell^2\xi \left( \frac{e^{-|\xi|y}}{|\xi|} - \frac{e^{-\gamma y}}{\gamma} \right) h^*(\xi) \tag{22}$$

with  $\gamma \equiv \gamma(\xi) = \sqrt{\ell^{-2} + \xi^2}$ . Accordingly, using (2) and (3) the transformed shear stress  $\sigma_{yx}^*$  becomes

$$\sigma_{yx}^*(\xi, y) = \mu g_{yx}^*(\xi, y) h^*(\xi), \tag{23}$$

with

$$g_{yx}^*(\xi, y) = i \left[ \frac{(y\xi - \text{sgn}(\xi))}{1-\nu} e^{-|\xi|y} - 4\ell^2\xi(|\xi|e^{-|\xi|y} - \xi^2\gamma^{-1}e^{-\gamma y}) \right], \tag{24}$$

where  $\text{sgn}()$  is the signum function.

Moreover,  $h^*(\xi)$  is defined according to (20) and (21)<sub>1</sub> as

$$h^*(\xi) = \int_{-\infty}^{\infty} h(t)e^{i\xi t} dt = \sum_{j=1}^2 \int_{a_j}^{b_j} h_j(t)e^{i\xi t} dt. \tag{25}$$

Employing the inverse Fourier transform (21)<sub>2</sub> in conjunction with (25) and reversing the order of integration, the shear stress  $\sigma_{yx}$  can be written as

$$\sigma_{yx}(x, y) = \frac{1}{2\pi} \int_{-\infty}^{\infty} \sigma_{yx}^* e^{-i\xi x} d\xi = \frac{\mu}{\pi} \sum_{j=1}^2 \int_{a_j}^{b_j} G_{yx}(x-t, y) h_j(t) dt + S, \quad (26)$$

where the kernel  $G_{yx}(x-t, y)$  is evaluated analytically as

$$G_{yx}(x, y) = \frac{1}{2} \int_{-\infty}^{\infty} g_{yx}^*(\xi, y) e^{-i\xi x} d\xi = \frac{x(y^2 - x^2)}{(1-\nu)r^4} + \frac{8\ell^2 x(x^2 - 3y^2)}{r^6} + 4\ell^2 \partial_x^3 K_0\left[\frac{r}{\ell}\right], \quad (27)$$

and  $K_n[\cdot]$  is the modified Bessel function of the second kind and  $n$ -th order. Using the same procedure, all the stress and couple-stress components are derived in *closed form* in the [Appendix](#).

#### 4. Singular integral equation approach

The unknown density function will be now determined by employing the method of singular integral equations (SIEs). In classical elasticity, the general procedure of reducing mixed boundary value problems to singular integral equations is given, e.g., by Erdogan [1978]. An application of the technique within the context of couple-stress elasticity for crack problems can be found in [Gourgiotis and Georgiadis 2008; 2007], and for contact problems in [Zisis et al. 2014; 2015; Gourgiotis et al. 2016; Karuriya and Bhandakkar 2017; Song et al. 2017; Wang et al. 2018].

The requirement that the crack-faces are free of shear tractions (see (14)) in the disjoint intervals  $(a_1, b_1)$  and  $(a_2, b_2)$  leads to the following system of coupled integral equations for the unknown densities  $h_j(t)$  ( $j = 1, 2$ ):

$$\int_{a_1}^{b_1} G_{yx}(x-t, 0) h_1(t) dt + \int_{a_2}^{b_2} G_{yx}(x-t, 0) h_2(t) dt = -\frac{\pi S}{\mu}, \quad x \in \mathcal{L}. \quad (28)$$

Moreover, to ensure uniqueness of the crack problem the following closure conditions must be satisfied:

$$\int_{a_1}^{b_1} h_1(t) dt = 0 \quad \text{and} \quad \int_{a_2}^{b_2} h_2(t) dt = 0. \quad (29)$$

For the solution of the coupled system of integral equations (28), it is expedient to separate the kernel to its singular and regular parts. To this purpose, we examine the asymptotic behavior of  $G_{yx}(x-t, 0)$  as  $x \rightarrow t$ . Using asymptotic analysis, we may readily write

$$G_{yx}(x-t, 0) = -\frac{(3-2\nu)}{(1-\nu)} \frac{1}{x-t} + R(x-t), \quad (30)$$

where the regular square-integrable kernel  $R(x-t)$  is given as

$$R(x-t) = \frac{4}{x-t} \left( \frac{1}{2} + \frac{2\ell^2}{(x-t)^2} - K_2\left[\frac{|x-t|}{\ell}\right] \right) - \frac{4 \operatorname{sgn}(x-t)}{\ell} K_1\left[\frac{|x-t|}{\ell}\right], \quad (31)$$

which is bounded as  $x \rightarrow t$ .

In view of the above, the following system of SIEs is obtained for the interaction problem of two colinear shear cracks in couple-stress elasticity:

$$-\frac{(3-2\nu)}{(1-\nu)} \sum_{j=1}^2 \int_{a_j}^{b_j} \frac{h_j(t)}{x-t} dt + \sum_{j=1}^2 \int_{a_j}^{b_j} h_j(t) R(x-t) dt = -\frac{\pi S}{\mu}, \quad x \in \mathcal{L}. \quad (32)$$

It is worth noting that in classical elasticity, the mode II and mode I interaction problems are governed by the same system of SIEs, i.e.,

$$-\frac{1}{(1-\nu)} \sum_{j=1}^2 \int_{a_j}^{b_j} \frac{h_j(t)}{x-t} dt = -\frac{\pi S}{\mu}, \quad x \in \mathcal{L}. \quad (33)$$

However, as it was shown in [Gourgiotis and Georgiadis 2008], in couple-stress elasticity the opening modes are more involved than the shear modes since additional densities must be introduced in order to satisfy the boundary conditions at the crack-faces.

To render the system of SIEs amenable to numerical treatment, the following normalizations are adopted [Erdogan and Wu 1993]:

$$\begin{aligned} x &= \frac{1}{2}(b_k - a_k)\hat{x} + \frac{1}{2}(b_k + a_k), & a_k < x < b_k, & \quad -1 < \hat{x} < 1, \\ t &= \frac{1}{2}(b_j - a_j)\hat{t} + \frac{1}{2}(b_j + a_j), & a_j < t < b_j, & \quad -1 < \hat{t} < 1, \\ R(x-t) &= \mathcal{N}_{kj}(\hat{x}, \hat{t}), & a_k < x < b_k, & \quad a_j < t < b_j, \\ z_{kj} &= (b_j - a_j)^{-1}[(b_k - a_k)\hat{x} + b_k + a_k - b_j - a_j], & \mathcal{Q}_{kj}(\hat{x}, \hat{t}) &= (z_{kj} - \hat{t})^{-1}, \end{aligned} \quad (34)$$

with  $j = (1, 2)$  and  $k = (1, 2)$ .

Accordingly, the system in (32) assumes the following form

$$\begin{aligned} -\frac{(3-2\nu)}{(1-\nu)} \int_{-1}^1 \frac{h_k(\hat{t})}{\hat{x} - \hat{t}} d\hat{t} - \frac{(3-2\nu)}{(1-\nu)} \sum_{j=1}^2 \int_{-1}^1 \mathcal{Q}_{kj}(\hat{x}, \hat{t}) h_j(\hat{t}) d\hat{t} \\ + \sum_{j=1}^2 \frac{1}{2}(b_j - a_j) \int_{-1}^1 \mathcal{N}_{kj}(\hat{x}, \hat{t}) h_j(\hat{t}) d\hat{t} = -\frac{\pi S}{\mu}, \\ k = (1, 2), \quad -1 < \hat{x} < 1, \end{aligned} \quad (35)$$

where the prime indicates that the summation does not include the term corresponding to  $j = k$ .

Following [Gourgiotis and Georgiadis 2007], the unknown densities  $h_k(\hat{t})$  can be written as a product of a regular bounded function and a singular function characterizing the asymptotic behavior near the crack-tips. Within the framework of couple-stress elasticity, asymptotic analysis near a mode II crack-tip [Huang et al. 1997; Gourgiotis and Georgiadis 2007; 2011] showed that the crack-face sliding displacement has the same asymptotic behavior as in the classical LEFM. Such a behavior was also corroborated by the uniqueness theorem for crack problems in couple-stress elasticity which imposes the requirement of boundedness for crack-tip displacements [Grentzelou and Georgiadis 2005]. The densities can be



expressed now in the following form:

$$h_k(\hat{t}) = \frac{\chi_k(\hat{t})}{\sqrt{1 - \hat{t}^2}}, \quad -1 < \hat{t} < 1, \quad k = (1, 2), \tag{36}$$

where the  $\chi_k(\hat{t})$  are sufficiently smooth functions.

For the solution of the system of SIEs in (35), the standard Gauss–Chebyshev quadrature is employed. For details, the reader is referred to [Erdogan 1978; Gourgiotis and Georgiadis 2007; 2008]. The discretized form of the system of SIEs becomes

$$\begin{aligned} -\frac{(3-2\nu)}{(1-\nu)} \frac{\pi}{N} \sum_{i=1}^N \frac{\chi_k(\hat{t}_i)}{\hat{x}_m - \hat{t}_i} - \frac{(3-2\nu)}{(1-\nu)} \frac{\pi}{N} \sum_{j=1}^2 \sum_{i=1}^N \mathcal{D}_{kj}(\hat{x}_m, \hat{t}_i) \chi_k(\hat{t}_i) \\ + \frac{\pi}{N} \sum_{j=1}^2 \sum_{i=1}^N \frac{1}{2} (b_j - a_j) \mathcal{N}_{kj}(\hat{x}_m, \hat{t}_i) \chi_j(\hat{t}_i) = -\frac{\pi S}{\mu}, \quad k = (1, 2), \end{aligned} \tag{37}$$

where the integration points  $\hat{t}_i$  and collocation points  $\hat{x}_m$  are given respectively as

$$\begin{aligned} \hat{x}_m &= \cos(m\pi/N) && \text{with } m = 1, \dots, N-1, \\ \hat{t}_i &= \cos((2i-1)\pi/(2N)) && \text{with } i = 1, \dots, N. \end{aligned} \tag{38}$$

Equation (37) together with the auxiliary conditions (29) provide a  $2N$  algebraic system of equations with  $2N$  unknowns:  $\chi_1(\hat{t}_i)$  and  $\chi_2(\hat{t}_i)$  ( $i = 1, \dots, N$ ). From the solution of the system the densities  $h_k(t)$  are evaluated and then the stress and couple-stress components can be readily computed using (49)–(52).

### 5. Results and discussion

In what follows, numerical results are presented regarding the crack-face displacements, the stress intensity factors (SIFs) and the energy release rates (ERRs) of the shear cracks. All the results are presented in terms of the three microstructural ratios:  $\alpha/\ell$ ,  $\beta/\ell$ , and  $\delta/\ell$  (or combinations of them), where the geometrical parameters ( $\alpha$ ,  $\beta$ ,  $\delta$ ) are defined in (13). It is assumed that in all cases  $\beta > \alpha$ , which implies that the right crack is always larger than the left one. Our purpose is to examine the possible deviations from the predictions of classical LEFM when the lengths of the cracks and the separation length between them becomes comparable to the characteristic material length of couple-stress elasticity. Two configurations are examined:

- (i) a micro-macrocrack interaction where the ratio  $\beta/\alpha$  is large and  $\alpha/\ell$  is small, and
- (ii) a micro-microcrack interaction where the lengths of both cracks are comparable to the characteristic material length  $\ell$  of the couple-stress theory (i.e., both  $\alpha/\ell$  and  $\beta/\alpha$  are small).

**5.1. Crack-face displacements.** The crack-face sliding displacements for the two colinear shear cracks can be readily evaluated by integrating (19) and using (29). Figure 2 shows the influence of the ratio  $\alpha/\ell$  on the normalized sliding crack-face displacements of both cracks. It is remarked that as the crack lengths become comparable to the characteristic length  $\ell$ , the material exhibits a more stiff behavior, i.e.,

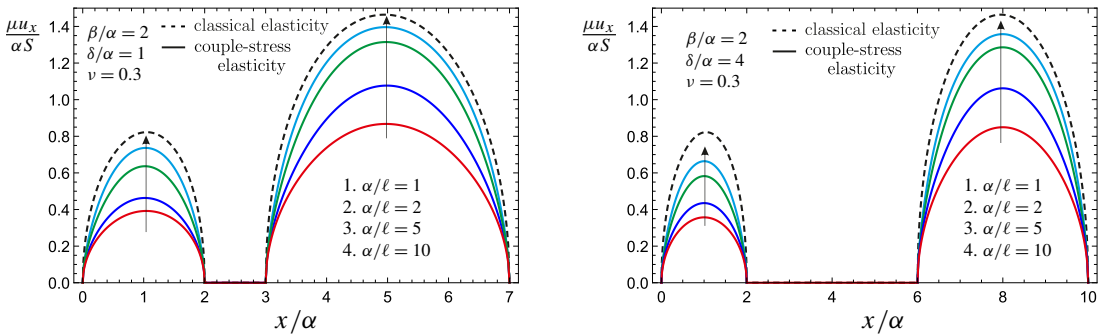


**Figure 2.** Variation of the normalized upper crack-face sliding displacement versus the normalized distance  $x/\alpha$  when (left) the distance between the cracks is  $\delta = \alpha$ , and (right) the distance between the cracks is  $\delta = 4\alpha$ . In all cases,  $\beta/\alpha = 2$  and  $\nu = 0.3$ .

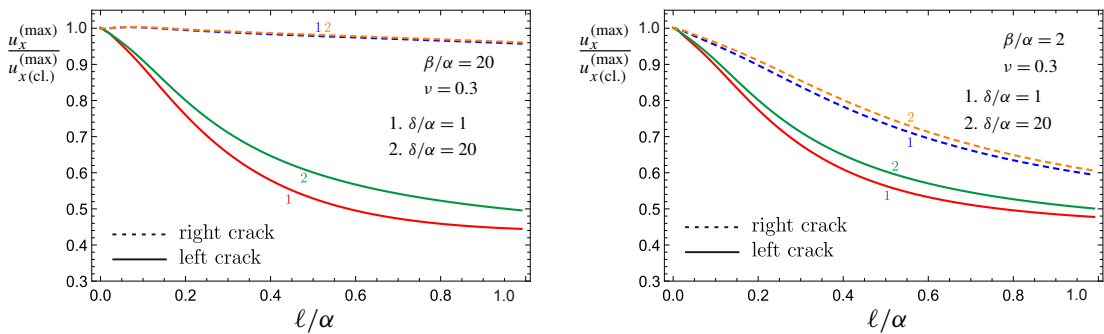


**Figure 3.** Variation of the ratio of the maximum sliding displacement in couple-stress and classical elasticity versus  $l/\alpha$  for (left)  $\beta/\alpha = 20$ , micro-macrocrack interaction, and (right)  $\beta/\alpha = 2$ , micro-microcrack interaction.

the crack-face displacements become smaller in magnitude as compared to the classical elasticity result (dashed line).

The stiffening effect is more clearly depicted in Figure 3 where the ratio of the maximum displacement in couple-stress elasticity  $u_x^{(max)}$  to the respective one in classical elasticity  $u_x^{(max)(cl.)}$  is plotted against  $l/\alpha$  for two different values of the geometric ratios  $\delta/\alpha$  and  $\beta/\alpha$ . It is observed that the decrease in the maximum couple-stress sliding displacement of the smaller (left) crack is more pronounced for higher values of the ratio  $\beta/\alpha$ , i.e., in the case of micro-macrocrack interaction and for smaller ratios  $\delta/\alpha$ . It is remarked further that for  $l/\alpha = 1$  the decrease in the maximum sliding displacement for the smaller crack can be up to 50% (Figure 3).

**5.2. Stress intensity factors.** The stress intensity factors (SIFs)  $K_{II}$  at the four crack-tips are defined as

$$K_{II}^{(a_k)} = \lim_{x \rightarrow a_k^-} \sqrt{2\pi(a_k - x)}\sigma_{yx} \quad \text{and} \quad K_{II}^{(b_k)} = \lim_{x \rightarrow b_k^+} \sqrt{2\pi(x - b_k)}\sigma_{yx}, \quad (39)$$

with  $k = (1, 2)$ . The dominant singular behavior of the shear stress in the vicinity of the crack-tips is due to the singular integrals in (26). Using standard asymptotic results regarding Cauchy-type integrals

[Muskhelishvili 1953], the near-tip shear stresses may be written as

$$\begin{aligned} \sigma_{yx}(x \rightarrow a_k^-, 0) &= -\frac{\mu(3-2\nu)}{\pi(1-\nu)} \lim_{\hat{x} \rightarrow -1^-} \int_{-1}^1 \frac{\chi_k(\hat{t})}{\sqrt{1-\hat{t}^2}(\hat{x}-\hat{t})} d\hat{t} \\ &= \frac{\mu(3-2\nu)}{(1-\nu)} \frac{\chi_k(-1)}{\sqrt{2}} (-1-\hat{x})^{-1/2}, \quad \hat{x} < -1, \end{aligned} \tag{40}$$

$$\begin{aligned} \sigma_{yx}(x \rightarrow b_k^+, 0) &= -\frac{\mu(3-2\nu)}{\pi(1-\nu)} \lim_{\hat{x} \rightarrow +1^+} \int_{-1}^1 \frac{\chi_k(\hat{t})}{\sqrt{1-\hat{t}^2}(\hat{x}-\hat{t})} d\hat{t} \\ &= -\frac{\mu(3-2\nu)}{(1-\nu)} \frac{\chi_k(+1)}{\sqrt{2}} (\hat{x}-1)^{-1/2}, \quad \hat{x} > 1, \end{aligned} \tag{41}$$

with  $k = (1, 2)$ .

Accordingly, the SIFs assume the following form

$$\begin{aligned} K_{II}^{(a_k)} &= \frac{\mu(3-2\nu)}{(1-\nu)} \sqrt{\frac{\pi(b_k - a_k)}{2}} \chi_k(-1), \quad k = (1, 2), \\ K_{II}^{(b_k)} &= -\frac{\mu(3-2\nu)}{(1-\nu)} \sqrt{\frac{\pi(b_k - a_k)}{2}} \chi_k(+1), \quad k = (1, 2). \end{aligned} \tag{42}$$

The values of the unknown densities at the crack-tips  $\chi_k(\pm 1)$  can be evaluated using Krenk’s interpolation technique [1975]. It is worth noting that in classical elasticity the SIFs are evaluated analytically for the case of two finite length colinear cracks (see, e.g., [Yokobori and Ichikawa 1967]). For the inner crack-tips  $(b_1, a_2)$ , the classical SIFs assume the following form:

$$\begin{aligned} K_{II\text{cl.}}^{(b_1)} &= \frac{\sqrt{2\pi}S}{2} \sqrt{\frac{b_2 - b_1}{(a_2 - b_1)(b_1 - a_1)}} ((b_1 - a_1) - (a_2 - a_1)f(m)), \\ K_{II\text{cl.}}^{(a_2)} &= \frac{\sqrt{2\pi}S}{2} \sqrt{\frac{a_2 - a_1}{(b_2 - a_2)(a_2 - b_1)}} ((b_2 - a_2) - (b_2 - b_1)f(m)), \end{aligned} \tag{43}$$

with

$$f(m) = \frac{K[m] - E[m]}{K[m]}, \quad m = \sqrt{\frac{(b_2 - a_2)(b_1 - a_1)}{(b_2 - b_1)(a_2 - a_1)}}, \tag{44}$$

where  $K[m]$  and  $E[m]$  are the complete Elliptic integrals of the first and second kind with modulus  $m$ .

Figure 4 illustrates the variation of the normalized SIF  $K_{II}^{(a_2)}/K_{II}^{(N)}$  of the crack-tip  $a_2$  with respect to the normalized separation distance  $\delta/\alpha$  in couple-stress and classical elasticity.  $K_{II}^{(N)}$  is the nominal macrocrack SIF, i.e., the SIF that would prevail in the absence of the microcrack  $2\alpha$ . In classical elasticity the nominal SIF is  $K_{II}^{(N)} = S\sqrt{\pi\beta}$ . In the couple-stress case the nominal SIF depends also upon the microstructural ratio  $\alpha/\ell$  and is always higher than the classical one as it was shown in [Gourgiotis and Georgiadis 2007]. It is observed that the normalized SIF is always greater than unity which, in turn, implies that the presence of the microcrack amplifies the shear stresses at the inner tip ( $a_2$ ) of the macrocrack creating thus a stress aggravation effect. It is worth noting, however, that for smaller  $\alpha/\ell$  ratios, i.e., when the length of the microcrack becomes comparable to the material microstructure, this

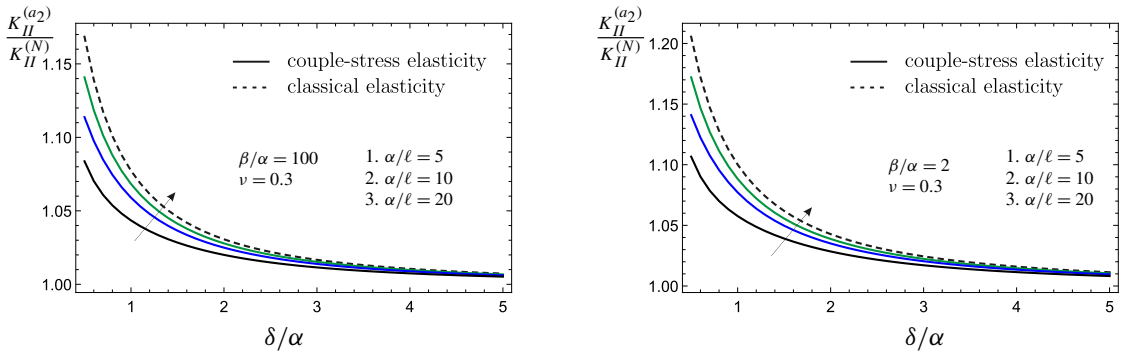


**Figure 4.** Variation of the normalized SIF  $K_{II}^{(a_2)}/K_{II}^{(N)}$  of the inner crack-tip  $a_2$  versus the normalized separation distance  $\delta/\alpha$  for various values of the microstructural ratio  $\alpha/\ell$ : (left)  $\beta/\alpha = 100$ , micro-macrocrack interaction, and (right)  $\beta/\alpha = 2$ , micro-microcrack interaction.

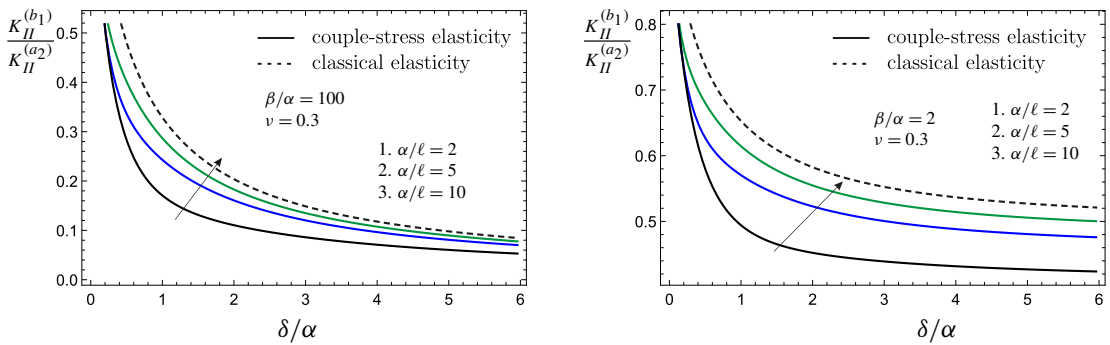


**Figure 5.** Variation of the ratio of the SIFs  $K_{II}^{(b_1)}/K_{II}^{(a_2)}$  of the inner crack-tips in couple-stress and in classical elasticity versus the normalized separation distance  $\delta/\alpha$  for various values of the microstructural ratio  $\alpha/\ell$ : (left)  $\beta/\alpha = 100$ , micro-macrocrack interaction, and (right)  $\beta/\alpha = 2$ , micro-microcrack interaction.

stress aggravation becomes less pronounced. Moreover, comparing Figure 4, left, with Figure 4, right, we note that:

- (i) the length of the larger crack does not affect significantly the variation of the normalized SIF, and
- (ii) that the interaction between the two cracks can be neglected when the separation distance is  $\delta > 5\alpha$ .

Figure 5 depicts the variation of the ratio of the SIFs  $K_{II}^{(b_1)}/K_{II}^{(a_2)}$  of the inner crack-tips:  $b_1$  (left crack) and  $a_2$  (right crack) with respect to the normalized separation distance  $\delta/\alpha$  for various microstructural ratios  $\alpha/\ell$ . Figure 5, left, shows the case of a micro-macrocrack interaction with  $\beta/\alpha = 100$ , while Figure 5, right, examines the case of a micro-microcrack interaction with  $\beta/\alpha = 2$ . The ratio is always below unity which shows that the crack propagation will be initiated from the tip of the largest crack. Moreover, in both cases, a significant decrease in the SIFs ratio is observed as compared to the classical elasticity result (dashed line) for decreasing values of  $\alpha/\ell$ . In light of the above and bearing also in mind that  $K_{II}^{(a_2)}$  decreases with increasing  $\ell/\alpha$  (see Figure 4), we may conclude that the effect of the larger

crack to the microcrack is less pronounced when couple-stress effects are taken into account. Finally, we note that as  $\ell/\alpha \rightarrow 0$  the SIFs ratio in couple-stress theory tends to its classical counterpart.

**5.3. Energy release rates.** The  $J$ -integral was first established in the context of couple-stress elasticity by Atkinson and Leppington [1974; 1977]. In the static case, the  $J$ -integral is identified as the energy release rate (ERR) and is path-independent [Lubarda and Markenscoff 2000]. For the evaluation of the ERR a rectangular shaped contour is considered centered at the crack-tip, with vanishing “height” along the  $y$ -direction and of length  $2\varepsilon$  [Freund 1990]. Letting  $\varepsilon \rightarrow 0$  allows us to use only the asymptotic near-tip fields. For the plane-strain case considered here, the  $J$ -integral assumes the following form [Gourgiotis et al. 2012]

$$\begin{aligned} J &= -2 \lim_{\varepsilon \rightarrow +0} \int_{c_t-\varepsilon}^{c_t+\varepsilon} \left\{ \sigma_{yy}(x, +0) \frac{\partial u_y(x, +0)}{\partial x} + \sigma_{yx}(x, +0) \frac{\partial u_x(x, +0)}{\partial x} + m_{yz}(x, +0) \frac{\partial \omega(x, +0)}{\partial x} \right\} dx \\ &= -2 \lim_{\varepsilon \rightarrow +0} \int_{c_t-\varepsilon}^{c_t+\varepsilon} \sigma_{yx}(x, +0) \frac{\partial u_x(x, +0)}{\partial x} dx, \end{aligned} \quad (45)$$

where  $c_t$  denotes the location of the crack-tip, i.e.,  $c_t = \{a_1, b_1, a_2, b_2\}$ . Note that the normal stress  $\sigma_{yy}(x, \pm 0)$  and the couple-stress  $m_{yz}(x, \pm 0)$  are zero along the whole crack line ( $y = 0$ ) for the shear mode case.

Now, by utilizing the asymptotic solutions (40) and (41) in conjunction with (20) and (36) and Fisher’s theorem for products of singular distributions (see, e.g., [Georgiadis 2003; Gourgiotis et al. 2012; Gourgiotis and Piccolroaz 2014]), we derive the final expressions for the ERRs in couple-stress elasticity:

$$\begin{aligned} J_{II} &= \frac{\mu(3-2\nu)}{2(1-\nu)} \frac{\pi(b_k - a_k)}{2} \chi_k^2(-1) \text{ at crack-tip } a_k, \quad k = (1, 2), \\ J_{II} &= \frac{\mu(3-2\nu)}{2(1-\nu)} \frac{\pi(b_k - a_k)}{2} \chi_k^2(+1) \text{ at crack-tip } b_k, \quad k = (1, 2). \end{aligned} \quad (46)$$

Comparing the above results with (42), the following relations can be established connecting the SIFs and the ERRs in couple-stress plane-strain elasticity

$$J_{II} = \frac{(1-\nu)}{2\mu(3-2\nu)} K_{II}^2, \quad (47)$$

while the respective relation in classical LEFM is

$$J_{II}^{(cl.)} = \frac{(1-\nu)}{2\mu} K_{II}^{(cl.)2}. \quad (48)$$

The variation of the ratio of the ERR in couple-stress theory to the respective one in the classical theory is shown in Figure 6 with respect to the microstructural ratio  $\ell/\alpha$  for a constant separation distance  $\delta = 2\alpha$ . The inner crack-tips  $b_1$  and  $a_2$  of the two colinear shear cracks are examined. It is observed that in all cases, the ratio  $J_{II}/J_{II}^{(cl.)}$  tends to unity when the characteristic material length tends to zero,  $\ell \rightarrow 0$ . This finding shows that the couple-stress solution converges to the classical one when the material microstructure is not considered. On the other hand, when  $\ell \neq 0$ , the ratio  $J_{II}/J_{II}^{(cl.)}$  decreases monotonically with increasing values of  $\ell/\alpha$  which implies that the couple-stress theory predicts a *strengthening effect* since a reduction of the crack driving force takes place as the material microstructure becomes more pronounced.

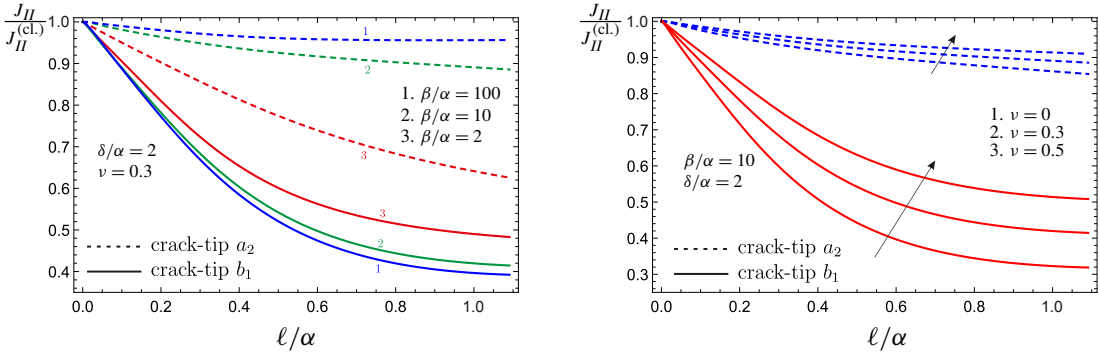


**Figure 6.** Variation of the ratio of the ERRs in couple-stress and classical elasticity versus the microstructural ratio  $\ell/\alpha$  for various values of (left)  $\beta/\alpha$ , and (right) the Poisson's ratio  $\nu$ . The inner crack-tips  $b_1$  (solid lines) and  $a_2$  (dashed lines) are examined.

More specifically, it is noted that in the case of the micro-macrocrack interaction,  $\beta/\alpha = 100$  (Figure 6, left), the ERR at the tip  $b_1$  of the microcrack (blue solid line) decreases significantly as compared to its classical counterpart for increasing ratios  $\ell/\alpha$ . On the other hand, couple-stresses have little effect on the ERR at the crack-tip  $a_2$  of the macrocrack (blue dashed line) as the ratio  $J_{II}/J_{II}^{(cl.)}$  remains close to unity for all values of  $\ell/\alpha$ . These findings show that:

- (i) the macrocrack strongly affects the behavior of the microcrack,
- (ii) the presence of the microstructure shields the microcrack, and
- (iii) the larger the macrocrack, the less significant the couple-stress effects are on its crack driving force.

Finally, regarding the effects of the Poisson's ratio, it is observed from Figure 6, right, that the strengthening effects are more pronounced for smaller values of  $\nu$ .

The influence of the normalized separation distance  $\delta/\alpha$  upon  $J_{II}/J_{II}^{(cl.)}$  is examined in Figure 7 for a micro-macrocrack configuration (Figure 7, left) and a micro-microcrack configuration (Figure 7, right). The strengthening of the microcrack due to the presence of the microstructure is observed also in this case. When the cracks are of comparable length (Figure 7, right) then there is a limiting separation distance above which the interaction between the microcracks can be neglected. For  $\beta = 2\alpha$  the limiting distance is  $\delta > 10\alpha$  (Figure 7, right — dashed lines). In this case, the cracks behave as single cracks in an infinite couple-stress material, a problem that has been previously studied by Gourgiotis and Georgiadis [2007].

The variation of the ratio of ERRs  $J_{II}/J_{II}^{(cl.)}$  with respect to  $\ell/\delta$  is illustrated in Figure 8 for various values of  $\beta/\alpha$  and a fixed ratio  $\delta/\alpha = 1$ . The inner crack-tips  $b_1$  and  $a_2$  are examined. It is observed that in the case of the micro-macrocrack interaction problem,  $\beta/\alpha = 100$  (blue lines), the ERR for the  $b_1$  crack-tip (blue solid line) suffers a significant decrease (compared to the classical value) as the separation distance becomes comparable to the material length  $\ell$ , highlighting again the fact that the macrocrack shields the microcrack further when the material microstructure is more pronounced. On the other hand, the decrease in the ERR is less significant when considering the  $a_2$  crack-tip of the macrocrack (dashed blue line) since the crack length is much larger than the material length scale. Note also that unlike the previous cases, the ratio is not monotonically decreasing for all values of  $\ell/\delta$ . Indeed, although the ratio experiences a decrease initially, then for  $\ell/\delta > 0.6$  it starts to gradually increase again, remaining however always below unity. A similar behavior is noted for the micro-microcrack interaction case,  $\beta/\alpha \leq 2$ , with

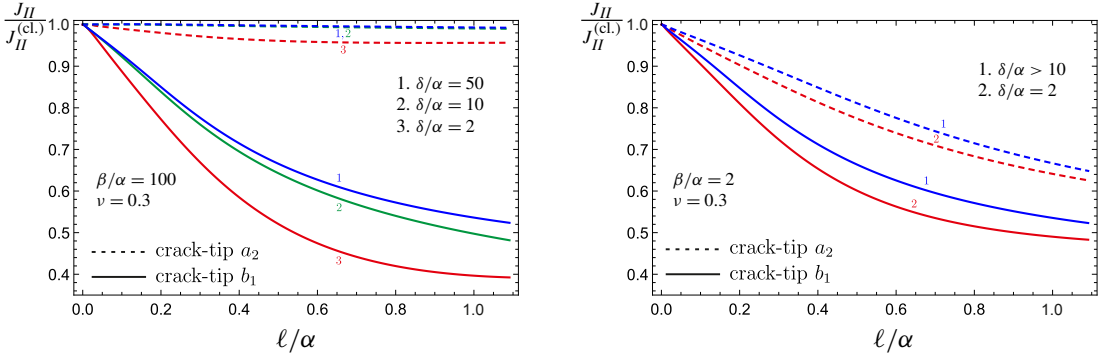


**Figure 7.** Variation of the ratio of the ERRs in couple-stress and classical elasticity versus the microstructural ratio  $\ell/\alpha$  for various values of the normalized separation distance  $\delta/\alpha$ : (left) micro-macrocrack interaction, and (right) micro-microcrack interaction. The inner crack-tips  $b_1$  (solid lines) and  $a_2$  (dashed lines) are examined.

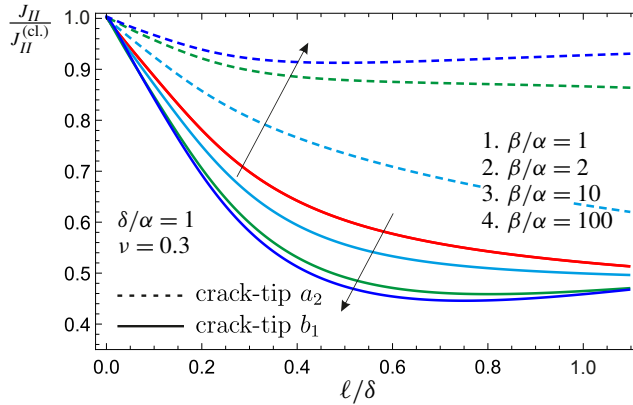


**Figure 8.** Variation of the ratio of the ERRs in couple-stress and classical elasticity versus  $\ell/\delta$  for various values of the geometrical ratio  $\beta/\alpha$ . The inner crack-tips  $b_1$  (solid lines) and  $a_2$  (dashed lines) are examined.

the smallest (left) crack suffering again the greatest decrease. In the case  $\beta/\alpha = 1$  both curves (red curve in Figure 8) coincide.

Figure 9 illustrates the variation of the normalized ERR,  $J_{II}/J_{II}^{(N)}$ , at the crack-tip  $b_1$  of the microcrack, with respect to the microstructural ratio  $\ell/\alpha$  in couple-stress elasticity (solid lines) and classical elasticity (dashed lines).  $J_{II}^{(N)}$  is the nominal microcrack ERR, i.e., the ERR that would prevail in the absence of the macrocrack.  $J_{II}^{(N)}$  can be obtained from the current solution by letting  $\delta/\alpha \rightarrow \infty$ . Two cases are examined:

- (a) the micro-macrocrack interaction ( $\beta/\alpha = 100$ ), and
- (b) the micro-microcrack interaction ( $\beta/\alpha = 2$ ).

A significant aggravation of the ERR is observed in the micro-macrocrack case (irrespective of the theory employed) as the separation distance  $\delta$  becomes comparable to the microcrack length  $2\alpha$  (Figure 9, left). In classical elasticity (dashed lines), the ratio  $J_{II}/J_{II}^{(N)}$  remains constant since the classical solution does

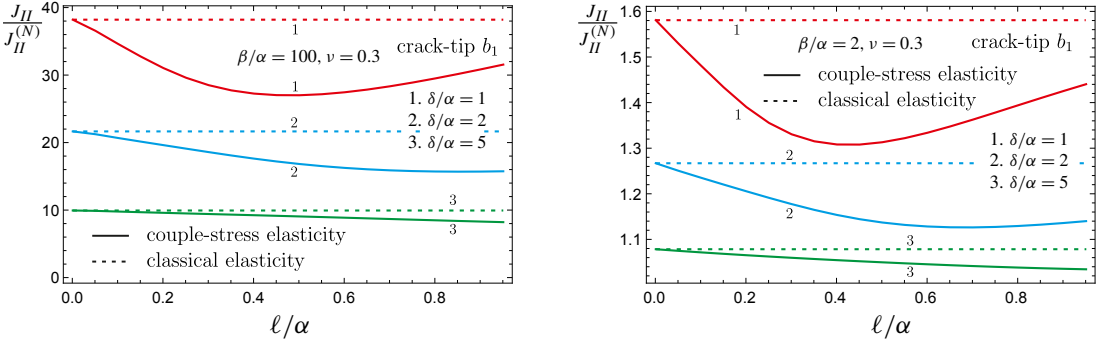


**Figure 9.** Variation of the normalized ERR at crack-tip  $b_1$  (small crack) versus the microstructural ratio  $\ell/\alpha$  for various values of  $\delta/\alpha$ : (left)  $\beta/\alpha = 100$ , and micro-macro crack interaction (right)  $\beta/\alpha = 2$ , micro-micro crack interaction.

not depend upon  $\ell$ . When couple-stress effects are taken into account, the ratio  $J_{II}/J_{II}^{(N)}$  decreases as compared to the classical result, which implies that the material microstructure shields the microcrack. The decrease is more pronounced for smaller separation distances and higher values of  $\ell/\alpha$ . A less pronounced decrease is observed if we examine the corresponding ratio for the  $\alpha_2$  crack tip of the macrocrack. In the micro-microcrack case ( $\beta/\alpha = 2$ , Figure 9, right), the effect of the larger crack ( $2\beta$ ) upon the smaller one ( $2\alpha$ ) is less significant (as expected) but the couple-stress effects are still dominant especially for small values of the ratio  $\delta/\alpha$ .

## 6. Conclusions

The interaction problem of two colinear shear cracks was investigated within the context of couple-stress elasticity. Two configurations which are of special interest were examined in detail: a micro-macrocrack interaction, and a micro-microcrack interaction. It was shown that significant deviations from the predictions of the classical LEFM are found when the geometrical parameters of the problem become comparable to the material length scale of couple-stress theory. Smaller crack-face displacements were observed when the crack-lengths become of the same order as the characteristic material length, corroborating thus the well-known stiffening effect that occurs in all gradient-type theories. As in the classical theory, the presence of the microcrack causes an aggravation of the SIF at the inner tip of the macrocrack. Nonetheless, this aggravation is less pronounced when couple-stress effects are taken into account. The couple-stress theory predicts also strengthening effects since a reduction of the crack driving force in both cracks takes place as the material microstructure becomes more distinct. Finally, it was found that the effect of the macrocrack on the microcrack becomes milder when couple-stresses are considered which verifies that the material microstructure shields the microcrack. The results obtained in the present study will enhance our understanding of the failure mechanisms that govern brittle materials and shed some light on the role of the microstructure in fracture on the microscale.

### Appendix: Stress and couple-stress components

The full-field expressions for the stress components  $\sigma_{pq}(x, y)$  and the couple-stress components  $m_{qz}(x, y)$  are derived by employing the inverse Fourier transform (21)<sub>2</sub> in conjunction with the definitions (25).



Reversing the order of integration, we readily obtain

$$\sigma_{pq} = \frac{1}{2\pi} \int_{-\infty}^{\infty} \sigma_{pq}^* e^{-i\xi x} d\xi = \frac{\mu}{\pi} \sum_{j=1}^2 \int_{a_j}^{b_j} G_{pq}(x-t, y) h_j(t) dt + S(1 - \delta_{pq}), \quad (49)$$

$$m_{qz} = \frac{1}{2\pi} \int_{-\infty}^{\infty} m_{pz}^* e^{-i\xi x} d\xi = \frac{\mu}{\pi} \sum_{j=1}^2 \int_{a_j}^{b_j} H_{qz}(x-t, y) h_j(t) dt, \quad (50)$$

where the indices  $p$  and  $q$  take the values  $\{x, y\}$  and  $\delta_{pq}$  is the Kronecker delta. The kernel functions  $G_{pq}$  and  $H_{qz}$  are evaluated in closed form as

$$G_{xx}(x, y) = \frac{y(3x^2 + y^2)}{(1-\nu)r^4} + \frac{8\ell^2 y(y^2 - 3x^2)}{r^6} - 4\ell^2 \partial_x^2 \partial_y K_0 \left[ \frac{r}{\ell} \right],$$

$$G_{yy}(x, y) = \frac{y(y^2 - x^2)}{(1-\nu)r^4} - \frac{8\ell^2 y(y^2 - 3x^2)}{r^6} + 4\ell^2 \partial_x^2 \partial_y K_0 \left[ \frac{r}{\ell} \right], \quad (51)$$

$$G_{xy}(x, y) = \frac{x(y^2 - x^2)}{(1-\nu)r^4} + \frac{8\ell^2 x(x^2 - 3y^2)}{r^6} - 4\ell^2 \partial_x \partial_y^2 K_0 \left[ \frac{r}{\ell} \right],$$

$$G_{yx}(x, y) = \frac{x(y^2 - x^2)}{(1-\nu)r^4} + \frac{8\ell^2 x(x^2 - 3y^2)}{r^6} + 4\ell^2 \partial_x^3 K_0 \left[ \frac{r}{\ell} \right],$$

$$H_{xz}(x, y) = \frac{4\ell^2 (y^2 - x^2)}{r^4} + 4\ell^2 \partial_x^2 K_0 \left[ \frac{r}{\ell} \right], \quad (52)$$

$$H_{yz}(x, y) = -\frac{8\ell^2 xy}{r^4} + 4\ell^2 \partial_x \partial_y K_0 \left[ \frac{r}{\ell} \right],$$

where  $r = \sqrt{x^2 + y^2}$ . Notice that the kernels in (49) and (50) are derived by replacing  $x$  with  $x - t$  in the above relations. Moreover, we note that the classical elasticity kernels are derived from the above equations by neglecting the terms that involve the characteristic length  $\ell$ .

## References

- [Anderson and Lakes 1994] W. B. Anderson and R. S. Lakes, “Size effects due to Cosserat elasticity and surface damage in closed-cell polymethacrylimide foam”, *J. Mater. Sci.* **29**:24 (1994), 6413–6419.
- [Atkinson 1984] B. K. Atkinson, “Subcritical crack growth in geological materials”, *J. Geophys. Res.* **89**:B6 (1984), 4077–4114.
- [Atkinson and Leppington 1974] C. Atkinson and F. G. Leppington, “Some calculations of the energy-release rate  $G$  for cracks in micropolar and couple-stress elastic media”, *Int. J. Fract.* **10**:4 (1974), 599–602.
- [Atkinson and Leppington 1977] C. Atkinson and F. G. Leppington, “The effect of couple stresses on the tip of a crack”, *Int. J. Solids Struct.* **13**:11 (1977), 1103–1122.
- [Baxevanakis et al. 2017] K. P. Baxevanakis, P. A. Gourgiotis, and H. G. Georgiadis, “Interaction of cracks with dislocations in couple-stress elasticity, II: Shear modes”, *Int. J. Solids Struct.* **118-119** (2017), 192–103.
- [Bigoni and Drugan 2007] D. Bigoni and W. J. Drugan, “Analytical derivation of Cosserat moduli via homogenization of heterogeneous elastic materials”, *J. Appl. Mech. (ASME)* **74**:4 (2007), 741–753.
- [Bigoni and Gourgiotis 2016] D. Bigoni and P. A. Gourgiotis, “Folding and faulting of an elastic continuum”, *Proc. R. Soc. Lond. A* **472**:2187 (2016), art. id. 20160018.

- [Deng and Nemat-Nasser 1994] H. Deng and S. Nemat-Nasser, “Microcrack interaction and shear fault failure”, *Int. J. Damage Mech.* **3**:1 (1994), 3–37.
- [Dyskin and Pasternak 2015] A. V. Dyskin and E. Pasternak, “Asymptotic analysis of fracture propagation in materials with rotating particles”, *Eng. Fract. Mech.* **150** (2015), 1–18.
- [Erdogan 1978] F. Erdogan, “Mixed boundary-value problems in mechanics”, pp. 1–86 in *Mechanics today, IV*, edited by S. Nemat-Nasser, Pergamon, Oxford, 1978.
- [Erdogan and Wu 1993] F. Erdogan and B. Wu, “Interface crack problems in layered orthotropic materials”, *J. Mech. Phys. Solids* **41**:5 (1993), 889–917.
- [Evans and Faber 1984] A. G. Evans and K. T. Faber, “Crack-growth resistance of microcracking brittle materials”, *J. Am. Ceram. Soc.* **67**:4 (1984), 255–260.
- [Freund 1990] L. B. Freund, *Dynamic fracture mechanics*, Cambridge Univ. Press, 1990.
- [Georgiadis 2003] H. G. Georgiadis, “The mode III crack problem in microstructured solids governed by dipolar gradient elasticity: static and dynamic analysis”, *J. Appl. Mech. (ASME)* **70**:4 (2003), 517–530.
- [Goodarzi et al. 2016] A. Goodarzi, M. Fotouhi, and H. M. Shodja, “Inverse scattering problem of reconstruction of an embedded micro-/nano-size scatterer within couple stress theory with micro inertia”, *Mech. Mater.* **103** (2016), 123–134.
- [Gourgiotis and Bigoni 2016a] P. A. Gourgiotis and D. Bigoni, “Stress channelling in extreme couple-stress materials, I: Strong ellipticity, wave propagation, ellipticity, and discontinuity relations”, *J. Mech. Phys. Solids* **88** (2016), 150–168.
- [Gourgiotis and Bigoni 2016b] P. A. Gourgiotis and D. Bigoni, “Stress channelling in extreme couple-stress materials, II: Localized folding vs faulting of a continuum in single and cross geometries”, *J. Mech. Phys. Solids* **88** (2016), 169–185.
- [Gourgiotis and Bigoni 2017] P. A. Gourgiotis and D. Bigoni, “The dynamics of folding instability in a constrained Cosserat medium”, *Phil. Trans. R. Soc. A* **375**:2093 (2017), art. id. 20160159.
- [Gourgiotis and Georgiadis 2007] P. A. Gourgiotis and H. G. Georgiadis, “Distributed dislocation approach for cracks in couple-stress elasticity: shear modes”, *Int. J. Fract.* **147**:1-4 (2007), 83–102.
- [Gourgiotis and Georgiadis 2008] P. A. Gourgiotis and H. G. Georgiadis, “An approach based on distributed dislocations and disclinations for crack problems in couple-stress elasticity”, *Int. J. Solids Struct.* **45**:21 (2008), 5521–5539.
- [Gourgiotis and Georgiadis 2011] P. A. Gourgiotis and H. G. Georgiadis, “The problem of sharp notch in couple-stress elasticity”, *Int. J. Solids Struct.* **48**:19 (2011), 2630–2641.
- [Gourgiotis and Piccolroaz 2014] P. A. Gourgiotis and A. Piccolroaz, “Steady-state propagation of a mode II crack in couple stress elasticity”, *Int. J. Fract.* **188**:2 (2014), 119–145.
- [Gourgiotis et al. 2012] P. A. Gourgiotis, H. G. Georgiadis, and M. D. Sifnaiou, “Couple-stress effects for the problem of a crack under concentrated shear loading”, *Math. Mech. Solids* **17**:5 (2012), 433–459.
- [Gourgiotis et al. 2016] P. A. Gourgiotis, T. Zisis, and K. Baxevanakis, “Analysis of the tilted flat punch in couple-stress elasticity”, *Int. J. Solids Struct.* **85-86** (2016), 34–43.
- [Grentzelou and Georgiadis 2005] C. G. Grentzelou and H. G. Georgiadis, “Uniqueness for plane crack problems in dipolar gradient elasticity and in couple-stress elasticity”, *Int. J. Solids Struct.* **42**:24-25 (2005), 6626–6244.
- [Hoagland et al. 1974] R. G. Hoagland, C. W. Marschall, A. R. Rosenfield, G. Hollenberg, and R. Ruh, “Microstructural factors influencing fracture toughness of hafnium titanate”, *Mater. Sci. Eng.* **15**:1 (1974), 51–62.
- [Huang et al. 1997] Y. Huang, L. Zhang, T. F. Guo, and K.-C. Hwang, “Mixed mode near-tip fields for cracks in materials with strain-gradient effects”, *J. Mech. Phys. Solids* **45**:3 (1997), 439–465.
- [Kachanov 1993] M. Kachanov, “Elastic solids with many cracks and related problems”, *Adv. Appl. Mech.* **30** (1993), 259–445.
- [Karuriya and Bhandakkar 2017] A. N. Karuriya and T. K. Bhandakkar, “Plane strain indentation on finite thickness bonded layer in couple stress elasticity”, *Int. J. Solids Struct.* **108** (2017), 275–288.
- [Koiter 1964] W. T. Koiter, “Couple-stresses in the theory of elasticity, I, II”, *P. K. Ned. Akad. Wetensc. B* **67** (1964), 17–44.
- [Kreher and Pompe 1981] W. Kreher and W. Pompe, “Increased fracture toughness of ceramics by energy-dissipative mechanisms”, *J. Mater. Sci.* **16**:3 (1981), 694–706.

- [Krenk 1975] S. Krenk, “On the use of the interpolation polynomial for solutions of singular integral equations”, *Quart. Appl. Math.* **32** (1975), 479–484.
- [Lakes 1983] R. Lakes, “Size effects and micromechanics of a porous solid”, *J. Mater. Sci.* **18**:9 (1983), 2572–2580.
- [Lakes 2016] R. S. Lakes, “Physical meaning of elastic constants in Cosserat, void, and microstretch elasticity”, *J. Mech. Mater. Struct.* **11**:3 (2016), 217–229.
- [Lakes 2018] R. S. Lakes, “Stability of Cosserat solids: size effects, ellipticity and waves”, *J. Mech. Mater. Struct.* **13**:1 (2018), 83–91.
- [Lubarda and Markenscoff 2000] V. A. Lubarda and X. Markenscoff, “Conservation integrals in couple stress elasticity”, *J. Mech. Phys. Solids* **48**:3 (2000), 553–564.
- [Mindlin 1963] R. D. Mindlin, “Influence of couple-stresses on stress concentrations”, *Exp. Mech.* **3**:1 (1963), 1–7.
- [Mindlin and Tiersten 1962] R. D. Mindlin and H. F. Tiersten, “Effects of couple-stresses in linear elasticity”, *Arch. Ration. Mech. Anal.* **11** (1962), 415–448.
- [Morini et al. 2014] L. Morini, A. Piccolroaz, and G. Mishuris, “Remarks on the energy release rate for an antiplane moving crack in couple stress elasticity”, *Int. J. Solids Struct.* **51**:18 (2014), 3087–3100.
- [Muki and Sternberg 1965] R. Muki and E. Sternberg, “The influence of couple-stresses on singular stress concentrations in elastic solids”, *Z. Angew. Math. Phys.* **16** (1965), 611–648.
- [Muskhelishvili 1953] N. I. Muskhelishvili, *Singular integral equations*, Noordhoff, Groningen, 1953.
- [Nara et al. 2011] Y. Nara, P. G. Meredith, T. Yoneda, and K. Kaneko, “Influence of macro-fractures and micro-fractures on permeability and elastic wave velocities in basalt at elevated pressure”, *Tectonophysics*. **503**:1-2 (2011), 52–59.
- [Noselli et al. 2013] G. Noselli, V. S. Deshpande, and N. A. Fleck, “An analysis of competing toughening mechanisms in layered and particulate solids”, *Int. J. Fract.* **183**:2 (2013), 241–258.
- [Piccolroaz and Movchan 2014] A. Piccolroaz and A. B. Movchan, “Dispersion and localisation in structured Rayleigh beams”, *Int. J. Solids Struct.* **51**:25-26 (2014), 4452–4461.
- [Piccolroaz et al. 2012] A. Piccolroaz, G. Mishuris, and E. Radi, “Mode III interfacial crack in the presence of couple-stress elastic materials”, *Eng. Fract. Mech.* **80** (2012), 60–71.
- [Radi 2008] E. Radi, “On the effects of characteristic lengths in bending and torsion on Mode III crack in couple stress elasticity”, *Int. J. Solids Struct.* **45**:10 (2008), 3033–3058.
- [Rice et al. 1994] R. W. Rice, C. C. Wu, and F. Borchelt, “Hardness–grain-size relations in ceramics”, *J. Am. Ceram. Soc.* **77**:10 (1994), 2539–2553.
- [Rose 1986] L. R. F. Rose, “Effective fracture toughness of microcracked materials”, *J. Am. Ceram. Soc.* **69**:3 (1986), 212–214.
- [Rubinstein 1985] A. A. Rubinstein, “Macrocrack interaction with semi-infinite microcrack array”, *Int. J. Fract.* **27**:2 (1985), 113–119.
- [Shao and Rudnicki 2000] J. F. Shao and J. W. Rudnicki, “A microcrack-based continuous damage model for brittle geomaterials”, *Mech. Mater.* **32**:10 (2000), 607–619.
- [Song et al. 2017] H.-X. Song, L.-L. Ke, and Y.-S. Wang, “Sliding frictional contact analysis of an elastic solid with couple stresses”, *Int. J. Mech. Sci.* **133** (2017), 804–816.
- [Sternberg and Muki 1967] E. Sternberg and R. Muki, “The effect of couple-stresses on the stress concentration around a crack”, *Int. J. Solids Struct.* **3**:1 (1967), 69–95.
- [Toupin 1962] R. A. Toupin, “Elastic materials with couple-stresses”, *Arch. Ration. Mech. Anal.* **11** (1962), 385–414.
- [Wang et al. 2017] C. D. Wang, P. J. Wei, P. Zhang, and Y. Q. Li, “Influences of a visco-elastically supported boundary on reflected waves in a couple-stress elastic half-space”, *Arch. Mech. Stos.* **69**:2 (2017), 131–156.
- [Wang et al. 2018] Y. Wang, H. Shen, X. Zhang, B. Zhang, J. Liu, and X. Li, “Semi-analytical study of microscopic two-dimensional partial slip contact problem within the framework of couple stress elasticity: cylindrical indenter”, *Int. J. Solids Struct.* **138** (2018), 76–86.
- [Yokobori and Ichikawa 1967] T. Yokobori and M. Ichikawa, “The interaction of parallel elastic cracks and parallel slip bands respectively based on the concept of continuous distribution of dislocations, II”, *Rep. Res. Inst. Strength Fract. Mater.* **3**:1 (1967), 15–37.

- [Zisis 2018] T. Zisis, “Anti-plane loading of microstructured materials in the context of couple stress theory of elasticity: half-planes and layers”, *Arch. Appl. Mech.* **88**:1-2 (2018), 97–110.
- [Zisis et al. 2014] T. Zisis, P. A. Gourgiotis, K. P. Baxevanakis, and H. Georgiadis, “Some basic contact problems in couple stress elasticity”, *Int. J. Solids Struct.* **51**:11-12 (2014), 2084–2095.
- [Zisis et al. 2015] T. Zisis, P. A. Gourgiotis, and F. Dal Corso, “A contact problem in couple stress thermoelasticity: the indentation by a hot flat punch”, *Int. J. Solids Struct.* **63** (2015), 226–239.

Received 12 Apr 2018. Accepted 20 Apr 2018.

PANOS A. GOURGIOTIS: [panagiotis.gourgiotis@durham.ac.uk](mailto:panagiotis.gourgiotis@durham.ac.uk)  
*Department of Engineering, Durham University, Durham, United Kingdom*

# JOURNAL OF MECHANICS OF MATERIALS AND STRUCTURES

[msp.org/jomms](http://msp.org/jomms)

Founded by Charles R. Steele and Marie-Louise Steele

## EDITORIAL BOARD

ADAIR R. AGUIAR	University of São Paulo at São Carlos, Brazil
KATIA BERTOLDI	Harvard University, USA
DAVIDE BIGONI	University of Trento, Italy
MAENGHYO CHO	Seoul National University, Korea
HUILING DUAN	Beijing University
YIBIN FU	Keele University, UK
IWONA JASIUK	University of Illinois at Urbana-Champaign, USA
DENNIS KOCHMANN	ETH Zurich
MITSUTOSHI KURODA	Yamagata University, Japan
CHEE W. LIM	City University of Hong Kong
ZISHUN LIU	Xi'an Jiaotong University, China
THOMAS J. PENCE	Michigan State University, USA
GIANNI ROYER-CARFAGNI	Università degli studi di Parma, Italy
DAVID STEIGMANN	University of California at Berkeley, USA
PAUL STEINMANN	Friedrich-Alexander-Universität Erlangen-Nürnberg, Germany
KENJIRO TERADA	Tohoku University, Japan

## ADVISORY BOARD

J. P. CARTER	University of Sydney, Australia
D. H. HODGES	Georgia Institute of Technology, USA
J. HUTCHINSON	Harvard University, USA
D. PAMPLONA	Universidade Católica do Rio de Janeiro, Brazil
M. B. RUBIN	Technion, Haifa, Israel

**PRODUCTION** [production@msp.org](mailto:production@msp.org)

SILVIO LEVY Scientific Editor

---


See [msp.org/jomms](http://msp.org/jomms) for submission guidelines.

JoMMS (ISSN 1559-3959) at Mathematical Sciences Publishers, 798 Evans Hall #6840, c/o University of California, Berkeley, CA 94720-3840, is published in 10 issues a year. The subscription price for 2018 is US \$615/year for the electronic version, and \$775/year (+\$60, if shipping outside the US) for print and electronic. Subscriptions, requests for back issues, and changes of address should be sent to MSP.

---

JoMMS peer-review and production is managed by EditFLOW<sup>®</sup> from Mathematical Sciences Publishers.

PUBLISHED BY

 **mathematical sciences publishers**  
nonprofit scientific publishing

<http://msp.org/>

© 2018 Mathematical Sciences Publishers

- Formulas for the H/V ratio of Rayleigh waves in compressible prestressed hyperelastic half-spaces** PHAM CHI VINH, THANH TUAN TRAN, VU THI NGOC ANH and LE THI HUE 247
- Geometrical nonlinear dynamic analysis of tensegrity systems via the corotational formulation** XIAODONG FENG 263
- Shaft-hub press fit subjected to couples and radial forces: analytical evaluation of the shaft-hub detachment loading** ENRICO BERTOCCHI, LUCA LANZONI, SARA MANTOVANI, ENRICO RADI and ANTONIO STROZZI 283
- Approximate analysis of surface wave-structure interaction** NIHAL EGE, BARIŞ ERBAŞ, JULIUS KAPLUNOV and PETER WOOTTON 297
- Tuning stress concentrations through embedded functionally graded shells** XIAOBAO LI, YIWEI HUA, CHENYI ZHENG and CHANGWEN MI 311
- Circular-hole stress concentration analysis on glass-fiber-cotton reinforced MC-nylon** YOU RUI TAO, NING RUI LI and XU HAN 337
- Elastic moduli of boron nitride nanotubes based on finite element method** HOSSEIN HEMMATIAN, MOHAMMAD REZA ZAMANI and JAFAR ESKANDARI JAM 351
- Effect of interconnect linewidth on the evolution of intragranular microcracks due to surface diffusion in a gradient stress field and an electric field** LINYONG ZHOU, PEIZHEN HUANG and QIANG CHENG 365
- Uncertainty quantification and sensitivity analysis of material parameters in crystal plasticity finite element models** MIKHAIL KHADYKO, JACOB STURDY, STEPHANE DUMOULIN, LEIF RUNE HELLEVIK and ODD STURE HOPPERSTAD 379
- Interaction of shear cracks in microstructured materials modeled by couple-stress elasticity** PANOS A. GOURGIOTIS 401